NJC

PERSPECTIVE

View Article Online
View Journal | View Issue

Cite this: *New J. Chem.*, 2016, **40**, 4016

Nature-inspired optimization of hierarchical porous media for catalytic and separation processes

Panagiotis Trogadas,†[ab] Michael M. Nigra†[ab] and Marc-Olivier Coppens*[ab]

Received (in Montpellier, France) 1st December 2015,
Accepted 12th February 2016

DOI: 10.1039/c5nj03406j

www.rsc.org/njc

Hierarchical materials combining pore sizes of different length scales are highly important for catalysis and separation processes, where optimization of adsorption and transport properties is required. Nature can be an excellent guide to rational design, as it is full of hierarchical structures that are intrinsically scaling, efficient and robust. However, much of the "inspiration" from nature is, at present, empirical; considering the huge design space, we advocate a methodical, fundamental approach based on mechanistic features.

1. Introduction

There has been a surge in our ability to control the structure of porous materials at multiple length scales. Such hierarchically structured porous materials give us the opportunity to combine high surface area with large pore volume and tunable pore sizes; together with the ability to functionalize the pore surface, geometrical and chemical control at multiple scales comes within reach, in contrast to monomodal porous materials.[1–5] Hierarchically structured porous materials are attractive to a plethora of applications, such as catalysis, sensing, regenerative medicine, bio- and biomedical technology, energy conversion and storage.[2,6,7] Materials combining pore sizes of different length scales are especially important for catalysis and separation processes, where optimization of adsorption and transport properties is required. Nature can be used as the source of inspiration for the design of hierarchical porous materials, since the architecture of nature is dominated by hierarchical structures, which have evolved over the eons to be adept and sometimes optimal to carry out similar functions.

Here we discuss the opportunities offered by using a nature-inspired engineering approach to design hierarchical porous materials, leveraging progress in both synthesis and computational methods. With nature-inspired, we mean the use of fundamental

[a] *Department of Chemical Engineering, University College London, Torrington Place, London, WC1E 7JE, UK. E-mail: m.coppens@ucl.ac.uk*
[b] *EPSRC "Frontier Engineering" Centre for Nature Inspired Engineering, University College London, Torrington Place, London, WC1E 7JE, UK*
† Equal contributions.

Panagiotis Trogadas

Panagiotis Trogadas is Senior Researcher and Teaching Fellow at the Centre of Nature Inspired Engineering and Department of Chemical Engineering at UCL, since 2014. Upon completion of his doctorate studies at IIT, Chicago (Prof. V. Ramani), he has taken postdoctoral posts at Georgia Institute of Technology (Prof. T. Fuller) and TU Berlin (Prof. P. Strasser) from 2010 until 2014. Trogadas has authored several funded grant proposals and his research is focused on nature-inspired electrocatalysts and electrochemical devices.

Michael M. Nigra

Michael M. Nigra is Senior Research Associate in the Department of Chemical Engineering at UCL since 2014, after completing his PhD at UC Berkeley in Chemical Engineering under the supervision of Prof. Alexander Katz. He received BSc degrees from Carnegie Mellon University in Chemical Engineering and Biomedical Engineering in 2007. His research currently explores the effects of nanoconfinement on metallic and enzymatic active sites in catalysis.

mechanisms that underpin desired properties in natural systems, and which can be translated within the context of a technical application. It is challenging to translate insights gained from observing the complex architecture of natural materials into artificial materials that can operate under, often, different conditions. This translation of natural design blueprints requires a fundamental, mechanistic understanding of materials and interfaces ranging from the macro- to the nanoscale – a range that could extend over six to ten orders of magnitude.[8–11] The current computational capabilities, though, are unable to integrate into a single, atomistically resolved model, the physical mechanisms that act at such disparate length scales, all of which could affect the overall performance of the material.[11] Rather than resolving every single atom, the key is to uncover the essential structural, physical or chemical features in the natural model that underlie those extraordinary properties we wish to employ on artificial materials for technical purposes.

In this article, we focus on static materials, that is, materials whose structure does not considerably change over time. Biology is replete with flexible, dynamic materials that have the remarkable ability to self-heal and adapt to changes in the environment. Understanding and embracing the mechanisms behind such dynamic self-organizing properties, opens up even more opportunities in nature-inspired engineering, but is of even greater complexity. Such methods complement activities that employ biology, rather than only borrow from its underlying mechanisms, and include bio-templating, bio-mineralization and synthetic biology.[12–19] Design and manufacturing methods based on the latter are in their infancy. Much of the "inspiration" from nature is, at present, empirical; considering the huge design space, we advocate a methodical, fundamental approach based on mechanistic features. This approach does not pretend to copy nature in the narrow sense of biomimetics, but to employ just enough of the much more complicated biological model to instill similar performance in one or a few facets, when employed in the different parameter space accessible to the targeted technical application. This space is sometimes wider (temperatures, pressures, basic materials), and sometimes narrower (time scales, complexity), within the economic and environmental constraints of the envisioned application. Our manufacturing toolbox and scale of application is often vastly different. All this needs to be accounted for to obtain the best combination of nature-inspired and other methods. However, observing nature with engineering eyes can unravel hidden mechanisms and help us innovate, guiding us to different approaches, away from conventional pathways in the limited room for further optimization.

Fig. 1 Photographs of humpback whale flippers showing the scalloped leading edge formed by tubercles.[25] Reprinted from ref. 25 with permission from Elsevier.

Research on the hierarchical structure of biological materials has attracted a lot of interest over the years;[11,20] examples are wood, tendons, bone and nacre.[12–19,21–24] The majority of manmade hierarchical materials essentially imitate, visually or "intuitively" approximating the structure of various living organisms or biological materials. Such straightforward biomimicry may or may not be successful, and it rarely achieves the level of sophistication and tailored architecture of biological counterparts.

An example of this form of biomimicry is the use of the design of the flippers of humpback whales for wing-based structures such as the blades of wind turbines, watercrafts, aircrafts and windmills (Fig. 1).[25,26] Humpback whales use their mobile flippers for banking and turning; they have tubercles on their flippers, allowing them to make acrobatic maneuvers to catch their prey.[25,26] The tubercles increase the maximum lift and decrease drag, acting as passive flow control devices that enhance the performance and maneuverability of the flipper. The utilization of wind turbine blades based on the flippers' design proved to be beneficial, as the performance of wind turbine blades is affected by the angle between the blade and the incident wind;[25] the imitation of the flippers' external structure increased the operating angle from 11° to 17°, resulting in a 40% increase in performance.[25]

An example of inspiration from nature based on mechanistic features is the design of aerodynamic, anti-biofouling materials based on the external structure of the shark skin.[26,27] The shark skin consists of numerous denticles forming complex three-dimensional (3D) shapes that jut out from the soft skin beneath, and which are composed of an outer enameloid layer and an inner bone-like layer surrounding a pulp cavity (Fig. 2).[26–28] This nanostructure minimizes the surface area available for the adhesion of microorganisms, which, in turn, keeps the skin clean. A transparent plastic film, imitating the structure of shark skin, has been used on airplane wings minimizing the

Marc-Olivier Coppens

Marc-Olivier Coppens, FIChemE, is Ramsay Memorial Chair and Head of Department of Chemical Engineering at UCL, since 2012, after academic posts at Rensselaer (USA) and TU Delft (Netherlands). He is also Director of the EPSRC "Frontier Engineering" Centre for Nature Inspired Engineering. Coppens is internationally recognised for pioneering work on nature-inspired chemical engineering: learning from fundamental mechanisms behind desirable traits in nature to develop creative and effective solutions to engineering challenges.

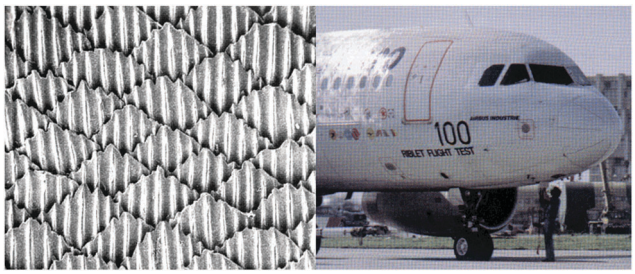

Fig. 2 The riblets on shark skin (left) provided the inspiration for the creation of a plastic film with the same microscopic texture used as coating for the airplane wings (right).[27] Copyright 1999, Rights Managed by Nature Publishing Group.

aircraft drag by 8% and thus reducing fuel consumption by 1.5%, while maintaining the surface of the aircraft clean.[27]

Yet a different example of borrowing from nature concerns the production of hierarchical titania photoanodes by using butterfly wings as templates to synthesize dye-sensitized solar cells. Here, biological material was directly used to confer the same hierarchical structure that was the reason for the blue or black color of the wings to the synthetic material; the result was a higher light-harvesting efficiency than a classical titania photoanode and a higher cell efficiency.[29]

As seen in these examples, fundamental understanding and utilization of the mechanistic basis is often missing in attempts to imitate biological systems, reducing bio-inspiration to biomimicry, copying presumably favorable features without clarity over which features are truly essential and which ones are superfluous, and without accounting for the many differences in other components or aspects of material and process design. We posit that to take optimal advantage of bio-inspiration in improving the design of functional materials, the relation between the structure and the function of a biological material has to be investigated, taking into account differences in context and constraints between the biological model and a technical application. This contribution discusses our nature-inspired chemical engineering (NICE) approach to providing solutions to engineering problems. We provide illustrations of this approach in the areas of diffusion and reaction in nanoporous media, hierarchically structured catalysts and fuel cells.

2. The nanoscale: nature-inspired confinement effects

One of the main aspects of our approach to nature-inspired engineering is to understand force-balancing mechanisms and apply them in new systems.[21] These forces are of many different types, such as electrostatic, van der Waals, hydrophobic/hydrophilic, and mechanical forces. Our first example is the encapsulation of catalytic active sites inside of porous media.

Nature's catalysts, enzymes, are known to be extremely efficient catalysts under very mild conditions. For many reactions in equivalent conditions, enzymes outperform synthetic catalysts by a wide margin, both in activity and selectivity. One of the challenges of using an enzyme as a catalyst is the separation of the catalyst from the reaction mixture. A possible solution to the problem of catalyst separation from the reaction mixture is to use a heterogeneous catalyst. The enzyme can be ''heterogenized'' by immobilization onto the catalyst support. The drawback to the immobilization of the enzyme is that its activity is often less than it was in solution. A possible explanation for this deactivation is that the support induces geometric changes to the enzyme upon immobilization, leading to functional groups moving out of place. However, there are some examples in the literature where catalytic activity is enhanced when the enzyme is immobilized, and two of them will be discussed in the next paragraphs.

GroEL/GroES chaperonin complexes in *E. coli* form a nanocage that helps single protein molecules to fold in isolation.[30–33] The group of Hartl and Hayer-Hartl showed convincingly that both the size of the cavity and the net-negative charge of the GroEL cage wall are essential to the folding mechanism and, thus, the function of the chaperonin. Inspired by this, Sang and Coppens immobilized enzymes on the internal surface of ordered mesoporous silica, SBA-15.[30] The underlying physico-chemical principle, borrowed from the biological model, is that both steric confinement and electrostatic force balancing are important in stabilizing the folded enzyme conformation. This principle can be realized without copying the complicated environment of the biological model. Sang and Coppens[30] used SBA-15,[34] because it is a material with a very high specific surface area and high pore volume, which, in addition, has a very narrowly distributed and easily tunable pore diameter in the range of, approximately, 5–15 nm. Conditions that result in high surface areas per unit mass include a lower hydrothermal aging time, and higher temperatures result in higher mesopore volumes.[35] This range is similar to the diameter of many enzymes. SBA-15 also has a low isoelectric point in aqueous solutions (around 2–3), lower than that of many enzymes, thus leading to electrostatic interactions at intermediate pH.

First, Sang *et al.* measured adsorption isotherms of enzymes on SBA-15 at their isoelectric points. This allowed them to determine the maximum pore loading for lysozyme, myoglobin, and bovine serum albumin in ordered mesoporous silica (SBA-15) and carbon (CMK-3). A geometric pore-filling model was proposed to explain the adsorption and packing of these enzymes in the mesopores. The model was validated by excellent agreement with experimental data.[36] Then, Sang and Coppens investigated the effects of changing the mesopore size on the catalytic activity of lysozyme and myoglobin for hydrolysis, respectively oxidation reactions, involving substrates and products that could easily diffuse in and out of the pores.[30] Fig. 3 illustrates the results of these catalytic studies, carried out in buffered solution at pH $\sim$ 7. A first conclusion is that the electrostatically immobilized enzyme is more active than the enzyme in solution. Additionally, as the pore diameter decreases and approaches the diameter of the enzyme, the activity increases, illustrating the effect of confinement in concave pores on the activity of the enzyme. The importance of surface curvature is further confirmed by comparing these results to work by Vertegel *et al.*, who showed that immobilization on the

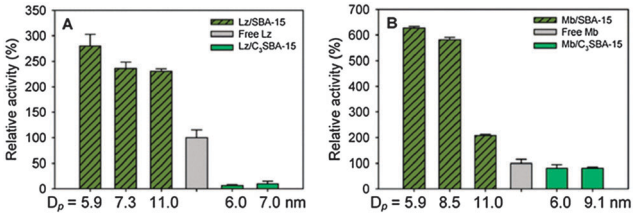

Fig. 3 Relative, intrinsic catalytic activities of enzymes immobilized on the surface of SBA-15 pores (green hashed bars), free in solution (grey bar), and inside of hydrophobic, propyl-modified SBA-15 pores (light green bars). Results are shown for a characteristic hydrolysis reaction catalyzed by lysozyme (A) and an oxidation reaction catalyzed by myoglobin (B).[30] Copyright 2011 Royal Society of Chemistry.

external, convex surface of silica nanoparticles leads to a decrease in catalytic activity.[37] To study the contribution of electrostatics to enzyme stabilization, the pore surface of the SBA-15 particles was functionalized with propyl chains, which screen the electrostatic interactions between the silica surface and the enzyme molecules, rendering the pore surface hydrophobic. As a result, the activity decreases significantly in the case of immobilized lysozyme when compared to free lysozyme in solution, which has a high isoelectric point (pI $\sim$ 11). For myoglobin, which has a lower pI $\sim$ 7.2, the activity remains similar to that in solution (Fig. 4).[30] This example demonstrates the importance of both steric and electrostatic confinement effects, similar to the GroEL/GroES chaperonin system. There are opportunities to study additional attributes of these immobilized enzyme systems, such as protective effects that pores may provide in harsh environments (temperature, proteases, strongly acidic/basic solutions), which are important to biotechnology as well as to applications in controlled drug delivery and sensing.[38]

Encouraged by these enhancements in catalytic activity, observed in immobilized enzymatic systems as described in the previous paragraph, rhodium (Rh) complexes were immobilized by anchoring on the pore surface of SBA-15. Conservation or enhancement of hydroformylation activity was also observed

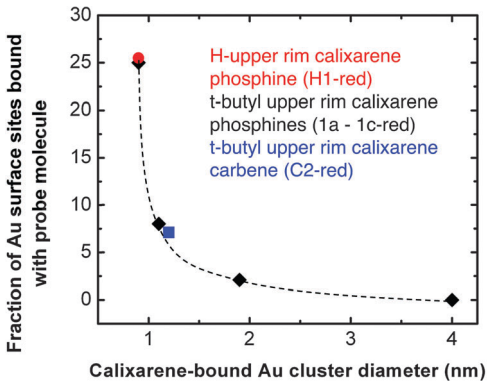

Fig. 4 Percentage of Au surface sites that are bound to a probe molecule as a function of gold cluster diameter using different calixarene ligands. The accessibility of the gold cluster surface is not controlled by the identity of bound calixarene ligand, but rather by the gold cluster size only, suggesting a mechanical model of accessibility.[45] Copyright 2013 Royal Society of Chemistry.

Table 1 1-Octene hydroformylation turnover frequencies for Rh-diphosphine catalysts both in solution and immobilized onto ordered porous silica SBA-15 and disordered porous silica gel. The range for SBA-15 indicates values measured with different samples, after up to 6 cycles of filtration and re-use[39]

Catalyst	TOF, mol product/(mol Rh h)
Rh diphosphine (homogeneous)	120
Rh diphosphine/SiO_2 gel	8
Rh diphosphine/SBA-15	101–195

when compared to the activity of the homogeneous Rh complex in solution.[39] Table 1 shows data for the hydroformylation of 1-octene with syngas at 50 bar and 80 °C in a batch reactor, after 23 hours. The study compared a homogeneous Rh diphosphine Xantphos complex and the same Rh diphosphine complex anchored to the surface of disordered, amorphous silica gel or anchored to the pore surface of ordered mesoporous SBA-15. The Rh complex immobilized on amorphous, disordered silica gel had the lowest activity, more than an order of magnitude below that of the homogeneous complex. The Rh complex anchored on the pores of SBA-15, on the other hand, was at least as active as the homogeneous complex, even after several cycles of catalyst filtering and re-use, while maintaining a similar high selectivity toward the desired linear aldehyde (linear/branched >30), and high catalytic stability. Equally promising results were also found at 20 bar. This illustrates the positive effects of controlled confinement in this catalytic system for 1-octene hydroformylation.[39] These results open a field of study into the effects of pore confinement on catalytic metal active sites.

Another method of creating confinement with the additional feature of pore functionalization is through silica imprinting. Using a nature-inspired approach, Katz and Davis reported a novel method creating substrate-specific cavities in amorphous silica that also left functional groups exposed after the removal of the templating molecule.[40] Enzymes are known for using different functional groups that modulate the activity of the active site. Further work by Katz and collaborators used silica imprinting techniques to generate microporous environments with isolated amine sites. The environment of the amine site was tuned with different acidity (through silanol groups) and different dielectric constant (through polar/nonpolar functional groups). Carbamate deprotection *via* thermolysis and the Henry reaction were studied with these materials. Structure–function relationships were proposed based on the environment surrounding the active site with the thermolysis or Henry reaction performance.[41]

The prior examples illustrate the effect of a porous environment on catalytic sites found inside pores. Can a simulated porous environment be constructed using organic molecules that are bound to a metal cluster surface? Can this porous environment around the metal cluster surface be used to tune the accessibility and electronic characteristics of the metal active sites as in enzymatic systems? One example of this work has been illustrated by Katz and co-workers using calixarene-bound gold clusters.[42–45] In these clusters, calixarenes are bound through functional groups such as phosphines on the lower rim to the surface of the gold clusters. Synthetically, a calixarene

phosphine or calixarene imidazolium salt reacts with dimethylsulfide gold(I) chloride to obtain a gold(I) calixarene complex.[43,45] These complexes are then reduced with $NaBH_4$, to obtain very small gold particles ranging in size from Au_{11} clusters to Au clusters approximately 2 nm in diameter. The size of the calixarene ligand at around 1 nm is approximately the same size as these clusters. Since the size of calixarene ligand is commensurate with the size of the gold clusters, a packing problem occurs on the surface of the gold nanoparticle. Only integer numbers of ligands can bind to the surface of the gold nanoparticle, and, with a small curved surface on these clusters, there are areas where another ligand does not have room to bind. This creates areas of accessible surface to which substrates can bind.[42–45] The number of accessible surface sites can be quantified with a titration procedure using strongly binding 2-napthalenethiol to count the number of sites. A correlation can be found linking gold cluster size and accessibility, as shown in Fig. 4. As the particle size becomes smaller and the ligand packing problem becomes more pronounced, the accessibility increases dramatically. The most accessible clusters used in this study were the Au_{11} clusters, which allowed for the binding of approximately three molecules on average per Au_{11} cluster.[43] The calixarene ligand is able to create pockets of accessibility on the gold nanoparticle surface for substrate binding. Additionally, the calixarene ligand, through the binding of its strongly donating phosphine groups, is able to tune the electronic state of the gold cluster, as illustrated by XPS results that indicated an electron-rich gold cluster surface.[43] This is similar to how functional groups are able to tune the activity around an enzymatic active site. These confined sites on the gold cluster surface with tunable electronic density should prove to be very interesting catalysts. More broadly, this approach of controlling accessibility as well as electronic tunability has great potential for the development of new and more active catalysts.

3. Bridging nano- and macro-scale: hierarchical transport networks in catalysis

Heterogeneous porous catalysts are often used in powder or pellet form in a fluid phase reactor, allowing for ease of separation and subsequent reuse or regeneration of the catalyst. In a process employing a porous catalyst, reactants must move from the bulk fluid stream into the catalyst and reach active sites on the, mostly internal, catalyst surface, and products should be transported from the active sites back to the bulk. A high specific, internal surface area is desirable to achieve a high concentration of active sites per unit catalyst mass. This often implies the use of nanoporous (micro- or mesoporous) catalysts. In the case of microporous catalysts like zeolites, molecularly-sized pores can, in addition, serve to control product distributions by size and shape selectivity. In nanopores, fluid transport is controlled by diffusion and is significantly slowed down with respect to transport in the bulk. To control product distributions and increase yields it is, therefore, important to control (usually, minimize) transport limitations. Catalyst pellet or particle size is typically dictated by reactor process conditions, such as pressure drop or reactor hydrodynamics, so that it rarely can be decreased at will. As a result, diffusion limitations are common in industrial processes.

One nature-inspired approach to decrease diffusion limitations is to use hierarchically structured porous materials with an optimized network of broad and narrow pores. Observations in nature can help to provide a mechanistic basis to find the optimal pore network architecture. Hierarchical transport networks are indeed common in many natural systems, such as the respiratory and circulatory systems, as well as in leaves. At large length scales transport is dominated by convective flow, while at smaller length scales transport is dominated by diffusion. This transition corresponds to a Péclet number of unity, $Pe \sim 1$. There is a quite sudden change in channel architecture at this transition: a fractal, broad power law distribution of channel diameters at large scales, where convection dominates, and a uniform distribution of narrow channels, where diffusion dominates. This type of architecture is remarkably universal in nature. It is witnessed in lungs (fractal upper airway tree, uniform channels in the alveoli), in trees (fractal tree crown and larger leaf veins, uniform distribution of small veins) and other biological transport networks. Simulations, discussed in Section 4, show that such architectures are optimal, hence a powerful basis for nature-inspired designs.

To synthesize these hierarchically structured porous materials, there is now a wide range of methods available, including dual, soft or hard templating, the Kirkendall effect, galvanic replacement and scaffolding. These techniques have been reviewed extensively elsewhere.[46–53] The templating approach is an effective and easily tuneable method to produce hierarchical porous particles, even though its major disadvantage is the post-processing techniques used for template removal. Calcination or chemical etching at high temperature result in the growth of particles, which destroys the pore solid architecture and porosity of the material.[47]

In the case of the dual templating approach, the simple mixing of two different structure-directing agents does not necessarily result in the synthesis of hierarchically structured materials.[54,55] The phase separation of mixed micelles, which is required to template distinct pore systems in hierarchical materials, only occurs when the free energy of mixing is positive.[56] An optimization of this method is needed that will prevent the mixing of numerous surfactants *via* trial and error until the final product is formed, to be able to predict the final outcome prior to the actual experiment. Recent, preliminary results demonstrate that the Flory–Huggins theory can be used as a theoretical tool to predict the phase separation behavior of mixed micelle template systems and help predict the formation of the hierarchical material that is templated by these micelles.[56] Specifically, the synthesis of hierarchical mesoporous silica using cetyltrimethylammonium bromide (CTAB) and *n*-octylamine (OA) as the dual template was predicted by the Flory–Huggins theory.[56] The critical micelle concentration values were experimentally determined to calculate the Flory–Huggins interaction parameter $\chi_{CTAB/OA}$ between those two surfactants. When $\chi_{CTAB/OA} > \chi_{critical}$, phase separation occurs

within the micellar phase, resulting in the formation of two micelles of different sizes (~1 and 17 nm) and, thus, in the synthesis of hierarchical silica consisting of worm-like and ordered mesopores.[56]

Hollow nanostructures can also be obtained *via* the Kirkendall effect and by using the galvanic replacement reaction. The former is based on mass transport through the interface between different solid phases, the latter on the electrochemical potential difference between the metals participating in the reaction.[47] On the contrary, scaffolding is a template-free method producing meso-/macroporous metal oxides and metals; however, during the deposition of these materials on surfaces, capillary flows currently obviate precise control over shape and size.[47]

The unique characteristics (large surface area, high meso-/macroporosity) of the resulting hierarchical nanomaterials transform them into ideal materials for catalysis, drug delivery and energy storage.[47]

4. Computationally guided optimization of the performance of hierarchically structured catalysts

4.1. Rational design guided by nature

The main disadvantages to consider when using a porous catalyst are diffusion limitations and catalyst deactivation by pore blockage, for example by coking, especially for reactions involving hydrocarbons.[57] Hierarchically structured catalysts can help to ease diffusion limitations in porous catalysts *via* a network of mesopores and macropores that provide ''molecular highways'' to access the active sites of the catalyst.[58,59]

The importance of a hierarchical pore network structure to mitigate effects of diffusion limitations and catalyst deactivation is well recognized in chemical reaction engineering. However, there is a significant divide[59] between, on the one hand, an extensive literature on materials synthesis, referred to in the previous Section, and, on the other hand, a large body of theoretical and computational work to predict how a multi-scale pore network architecture affects diffusion limited reactions.[60–65] Rational design should include all length scales, not only the nanoscale. This is no longer a distant dream, as increasing synthetic control over hierarchical porous materials architecture, together with sophisticated visualization methods to reveal the inner structure of (working) catalysts[66,67] opens up fresh opportunities for rational, multi-scale design, which should be informed by insights from theoretical methods and realistic multi-scale computational techniques. The range of reactions that would benefit from such an approach is huge, and includes, for example, deNO_x,[58] alkylation,[68,69] hydrodemetallation,[70] autothermal reforming,[71] decomposition of organic dye molecules,[72,73] Fisher–Tropsch,[2,74,75] esterification[76] and epoxidation[77] reactions.

It was mentioned earlier that many hierarchical transport networks in nature have a recurring architecture that consists of a fractal, self-similar geometry at relatively large length scales (macro-scale) and a uniform distribution of transport channels at smaller length scales (meso-scale), the transition occurring around Pe ~ 1. Is this a coincidence? If not, this could be a very simple, yet powerful, nature-inspired design principle. However, only global optimisation of transport and reaction problems can reveal the benefits of such structures. Comprehensive, global optimization from nano-to macro-scale has not yet been carried out, but separate studies at the mesoscale (diffusion control) and macroscale (convection control) suggest that natural architectures are indeed highly performing, if not optimal, also in the context of heterogeneous catalysis, as will now be discussed.

4.2. Nature-inspired structuring at the meso-scale

Gheorghiu and Coppens investigated the diffusion and subsequent first-order reaction in hierarchical bimodal porous catalysts with a given nanoporosity, the latter dictating the intrinsic catalytic and diffusion properties at the nanoscale.[78] In this study, the number of broad pores, acting as ''highways'' was gradually increased, and the global optimum of pore sizes and locations was compared to that of a fractal distribution and a uniform distribution in pore sizes and locations. The latter corresponds to a bidisperse porous catalyst. Two main conclusions resulted from this study. The first conclusion was that, for a given number of large pores, the optimized hierarchical catalyst had a higher effectiveness factor than the bidisperse catalyst, in which all wide pores have the same diameter and are uniformly spaced, meaning that a smaller mass of hierarchically porous catalytic material was sufficient to obtain the same catalytic yield as the catalyst with the uniquely sized wide pores. The second conclusion was that the optimal fractal network of pores was similar in effectiveness to the optimized bimodal pore network over all possible pore size distributions, indicating that fractal networks were already very much optimized for transport.[78]

Nevertheless, these simulations assumed a constant number of large pores. Relaxing this constraint, Wang *et al.* compared general bi-disperse and bi-modal broad pore size distributions in hierarchically structured catalysts, irrespective of the number of pores.[79] The nanoporous catalyst structure was again held constant in this comparison. The results show a large improvement of the bi-disperse and bimodal catalysts over the mono-disperse catalyst with only nanopores, but no significant difference in yields between the bi-disperse and bimodal catalysts. Note that these optimal structures could have different porosities. The optimal bi-disperse structure consists of nanoporous catalyst grains of a size that is such that the local effectiveness factor is close to 1, making optimal use of the internal structure for catalysis (the image of biological cells of optimal, constant size comes to mind); a somewhat larger size would lead to internal diffusion limitations. The optimal macro/mesoporosity balances a sufficiently high fraction of catalytically active, nanoporous material (reaction) with sufficient porosity (diffusion). The simulations show that this macro/mesoporosity matters more than the actual distribution of wide pore sizes around the optimal average wide pore size, which only has a secondary effect, hence the near-optimality of a unique wide pore size if the number of wide pores

can be large enough. If the latter condition is not satisfied, then a distribution of wide pore sizes may lead to better results, as shown by Gheorghiu and Coppens.[78] From an industrial synthesis point of view, these conclusions are fortuitous, as full control over a specific broad pore size distribution is harder than to mainly control the average macro/mesoporosity and average wide pore size, as well as the size of the nanoporous grains.[79] Pulsed-field gradient NMR experiments of 1-octane in a fluid catalytic cracking (FCC) catalyst illustrate that, at high temperatures relevant to FCC, the macro/mesoporosity has a much greater effect on the overall, effective diffusivity than the nanoporosity – the opposite of what happens at low temperatures, where intracrystalline diffusion, within the zeolite crystals, is limiting. As a result, increasing the mean mesopore size decreases the diffusion limitations.[80] At this point, it is interesting to note the similarity with biological systems where, as mentioned earlier, a uniform meso/macroporosity is found in the diffusion-limited regime in various tissues and leaves.

Wang and Coppens extended these conclusions to hierarchically structured porous catalysts for reactions with a general rate expression, deriving a general criterion for the calculation of the optimal effectiveness factor as a function of a modified, generalized Thiele modulus. This was applied to the selective catalytic reduction (SCR) of nitrogen oxides ($deNO_x$) in flue gas over a V_2O_5/TiO_2 catalyst.[58] For a typical washcoated SCR monolith, the optimized hierarchical catalyst layer was found to be 80–180% more active than the purely mesoporous catalyst while using 20–40% less material.[58,81,82] These results are consistent with the results from Gheorghiu and Coppens indicating that less catalyst mass would be needed in the case of the hierarchically structured catalysts *versus* the monodisperse porous catalyst.[78] Groen, *et al.* show by introducing mesopores into a ZSM-5 material *via* desilication, that the diffusion of neopentane is two orders of magnitude larger in the mesoporous–microporous *versus* the purely microporous zeolite material.[83] Another example from Choi, *et al.* illustrates an increase in activity of approximately 20-fold of a mesoporous MFI zeolite over bulk ZSM-5 zeolite for the synthesis of large molecules jasminaldehyde and vesidryl.[84]

In addition to heterogeneous catalysis, separations are another area where an optimized hierarchical design of porous materials can increase overall performance, for example in adsorbents, membranes and chromatography. Computational studies by Ye *et al.* show that adsorbents with a uniform spatial distribution of meso-/macroporosity maximize adsorption and desorption performance in cyclical operation (as in pressure swing adsorption), a similar result to what had been observed for catalysis; this was illustrated for the adsorption of *n*-pentane onto 5A zeolite materials.[85] The groups of Fajula and Galarneau[74] have shown how hierarchically structured silica monoliths with independent control of meso- and macroporosity can be prepared by using a combination of spinodal decomposition (to form a macroporous bicontinuous phase) and micellar templating (to form ordered mesoporous silica MCM-41). The macroporosity is preserved and disordered mesoporosity turned into ordered mesoporosity by using a pseudomorphic transformation to generate the MCM-41 inside the silica skeleton. Such hierarchical monoliths can be used for separations and catalysis.[74,75] Macroporous zeolite monoliths are often used in continuous flow microreactors for the removal of radioactive materials from aqueous effluents or for the denitrogenation of fuel feeds containing heavy heteroaromatic nitrogen and sulfur impurities.[86–88] These hierarchical catalysts exhibit high efficiency and increased productivity due to their mesoporous/macroporous structure and high surface area, which enhance mass transport and improve overall catalytic efficiency.[86–88] Our nature-inspired engineering approach suggests that monoliths with an optimized, uniform meso-/macroporosity should again lead to the highest performance, when diffusion is rate determining, although convective transport could benefit from a broader distribution in macroporosity; it would be worthwhile to calculate the optimal architecture and validate this approach experimentally.

Wang and Coppens also investigated autothermal reforming of methane with a hierarchically structured Ni/Al_2O_3 catalyst.[71] In this contribution, the authors varied the macropore size and the macroporosity while holding the mesoporosity constant. The results indicated that increases in activity of between 40–300% over a commercial catalyst are possible using a hierarchically structured catalyst by adjusting the size of the macropores and the macroporosity. The catalytic effectiveness factors were found to be the highest for a macropore size of $\sim$1 μm and a macroporosity of between 0.2 and 0.3. The effect of macroporosity on selectivity was also studied, showing that, at high macroporosities at conditions representative for the reactor inlet, more CO leaves the catalyst before being converted in the forward water–gas shift (WGS) reaction. For reaction conditions similar to the outlet, more hydrogen diffuses out of the catalyst before being consumed in the reverse WGS reaction.[71] Interestingly, the porosity can be used as a handle to control the H_2/CO ratio, without changing the intrinsic catalyst structure at the nanoscale.

Rao and Coppens computationally investigated hydrodemetallation to convert nickel metalloporphyrins to metal sulfides using a hierarchically structured catalyst.[70] This is an important reaction in refinery operations, which had also been studied by Keil and Rieckmann,[89,90] who already suggested the importance of a hierarchical catalyst structure with optimized mesoporosity. The catalyst is known to deactivate through the loss of active surface area and pore blocking. One significant feature of this work is that these calculations took into account catalyst deactivation due to the deposition of metals in both meso- and macropores and on the active sites, which is a real industrial problem when using porous heterogeneous catalysts. Building on Smith and Wei's work,[91] a random spheres model (RSM) approach was used to model the nanoporous features of the catalyst, while a 2D continuum model was used to model the other features of the catalyst. The mesoporosity was held constant for all systems, while the macroporosity profile was adjusted (Fig. 5). The calculations illustrated a 40% increase in useful lifetime of the hierarchically structured catalyst compared to a purely mesoporous catalyst, at the reactor scale. Additionally, 21% less catalyst mass is needed using the hierarchically structured catalyst over the purely mesoporous catalyst. That less

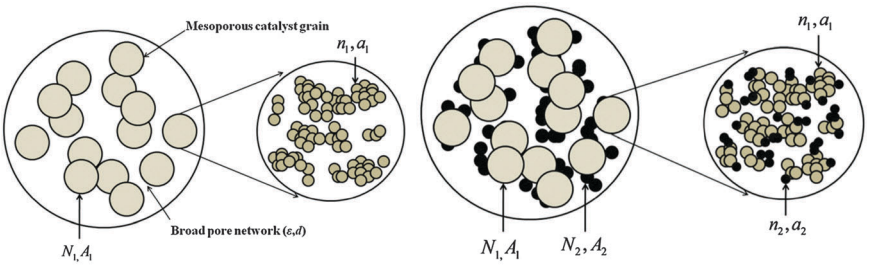

Fig. 5 Hierarchically structured catalyst with overlapping mesoporous grains (left). Broad macropores separate these mesoporous grains. The mesoporous grains are composed of overlapping catalyst spheres, with mesopores in between them (right). Hierarchically structured catalyst (same as left) with discrete spheres representing metal sulfide deposits that block the pores leading to catalyst deactivation.[70] Reprinted from ref. 70 with permission from Elsevier.

catalyst mass is needed is again consistent with previous results.[70] Further calculations were performed on this system, but also accounting for deactivation in the macropore network. The calculated value for the macroporosity of 29% is close in range to what was reported in the patent literature for a bimodal HDM/HDS catalyst.[70]

In another example of studying pore blockage in hierarchical materials, Ye *et al.* have investigated multiphase reactions inside of catalyst particles with a hierarchical pore structure using a discrete model.[92] Their calculations were compared with experimental results for the hydrogenation of benzene using a Pd/γ-Al_2O_3 catalyst. A common source of pore blockage is due to liquid that has not evaporated. This is a complex problem which combines mass transfer, phase change, and reaction kinetics into one system, all of which can contribute to the apparent reaction rate. The results indicate that pore blockage can account for up to 50% of the hysteresis loop area when determining the relationship between the reaction rate or effectiveness factor and the control variable. Changing the volume-averaged mean pore size did not produce significant pore blocking effects; however, changing the standard deviation of the pore size distribution or the pore network connectivity did show significant pore blocking effects.[92]

Recent work by Koekkoek *et al.* investigates benzene oxidation to phenol with nitrous oxide using a hierarchically structured Fe/ZSM-5 catalyst.[93] Using various synthesis methods, which include carbon templating, desilication, and organosilane templating, the authors report an increase in turnover frequency of up to a factor of 2 over the conventional Fe/ZSM-5 catalyst. These catalysts also exhibit slower deactivation characteristics than the conventional Fe/ZSM-5 catalyst.[93] Hartmann presented a review of the different synthesis methods of hierarchical zeolites and their catalytic applications in 1-octene and cyclohexene epoxidation as well as in isomerization of *n*-pentane and *n*-heptane. In these examples, the hierarchical zeolite catalyst outperformed the conventional zeolite catalyst in both activity and selectivity.[94] In another industrially relevant reaction, the ethylation of benzene, a hierarchical zeolite catalyst was used. It is believed that the shorter diffusion path in a hierarchical zeolite leads to less opportunity for further alkylation and thus higher selectivity for the hierarchical zeolite was observed *versus* the conventional zeolite.[94,95]

4.3. Nature-inspired structuring at the macro-scale

A representative example of a nature-inspired approach at the macro-scale is illustrated through the design of flow fields for proton exchange membrane fuel cells (PEMFCs). A nature-inspired chemical engineering (NICE) approach can aid towards achieving the low Pt loading target by modifying the PEMFC design guided by the hierarchical structure of the lung.[21,47,96,97]

The respiratory tract of a mammalian lung has a similar fractal structure consisting of many generations of branches, from the trachea to the bronchioles, in which flow dominates transport, followed by generations of space-filling acini lined by alveoli in which diffusion dominates transport.[21,47] Entropy production while breathing is uniformly distributed and globally minimized in both regimes, a very desirable property from the point of view of thermodynamic efficiency.[21,47] The fractal architecture of the upper part of the lung connects multiple microscopic elements to a single macroscopic element *via* equal hydraulic path lengths providing equal transport rates to or from the cells.[21,47] A great advantage of this fractal structure is its scalability. The fractal network can be broadened by adding a generation, while keeping the structure of the microscopic building units the same (Fig. 6).[21,47]

These observations can be used as a building principle for PEMFC flow field design;[21,47] Fig. 7 shows a two-dimensional fractal distributor built in-house, by stereo-lithography. Air or O_2 enters the distributor through a single inlet, flows through

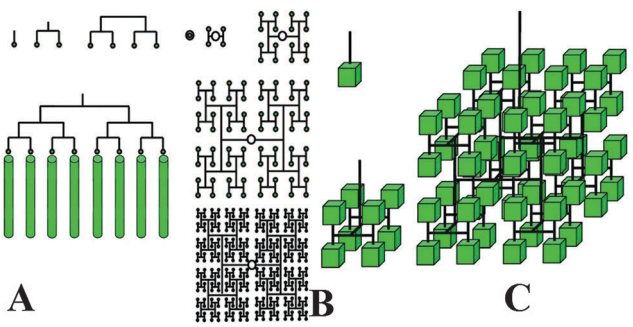

Fig. 6 (A) Set of 1D distributors feeding progressively larger 1D arrays (vectors); (B and C) extension of the scalable, fractal distributor concept to 2D and 3D, respectively.[47] Copyright 2015 Wiley.

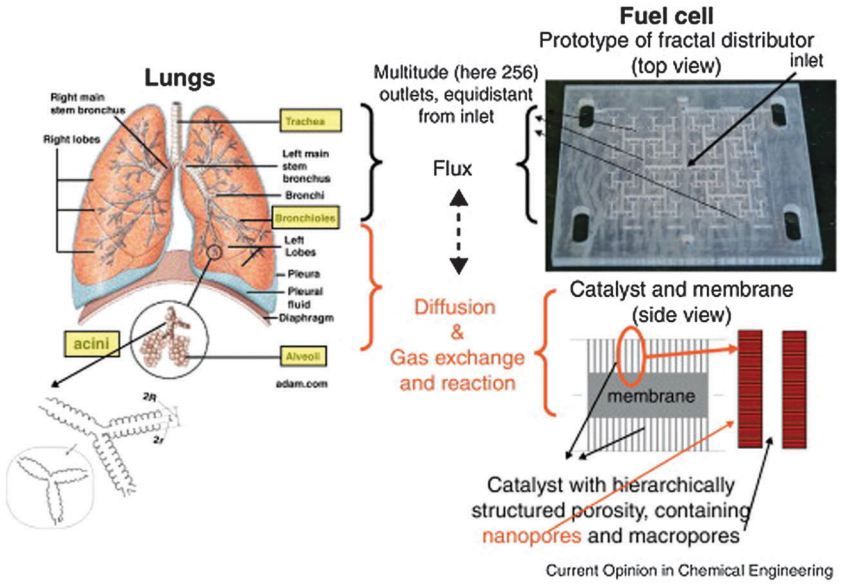

Fig. 7 Fuel cell design guided by the architecture of the lung and the associated physical mechanisms.[47] Copyright 2015 Wiley.

the branching channels and exits the distributor through a square array of outlets, which have the same hydraulic distance from the inlet. As a result, this fractal distributor uniformly feeds O_2 to the catalyst layer, while produced water is removed *via* an embedded collector, circumventing the non-uniformity issues of other flow-field geometries.[47]

Initial modeling studies on the effect of the fractal distributor on the fuel cell performance and gas distribution have been carried out.[98] Fractal distributors with 16, 64 and 256 outlets have been reported in the literature (Fig. 8). A fractal distributor with 256 channels exhibited 200% and 50% higher power generation than distributors with 16 and 64 channels, respectively (Fig. 9), due to the uniform flow distribution on the catalyst layer and low pressure drop produced in these flow patterns, resulting in enhanced flow rates of oxidants.[98]

Even though these preliminary modeling results on the effect of a fractal distributor on fuel cell performance are encouraging, the main challenge is the manufacturing of the bipolar plates, since the task of machining such an intricate design is complex at sub-mm level, which could lead to failures in the current collector material. These issues should be increasingly addressed by the current, rapid progress in micromachining and additive manufacturing methods.

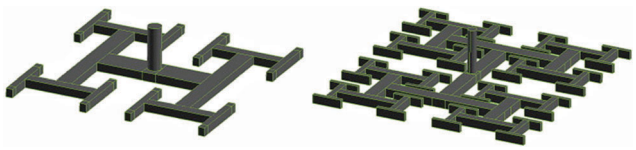

Fig. 8 Fractal design with 16 and 64 outlets used for modeling studies.[98] Reprinted from ref. 98 with permission from Elsevier.

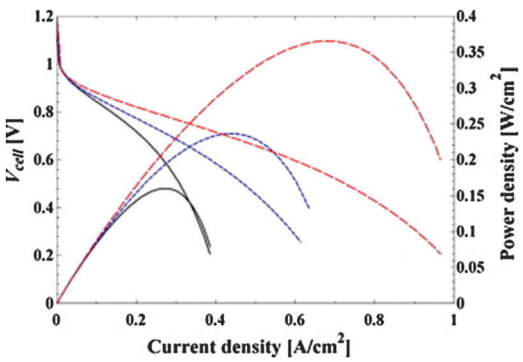

Fig. 9 PEMFC performance when fractal distributors are used as bipolar plates: (black line – 16 branches; blue line – 64 branches and black line – 256 branches).[98] Reprinted from ref. 98 with permission from Elsevier.

5. Conclusion and perspectives

It is crucial to improve the design of hierarchical porous materials for applications in catalytic and separation processes. In-depth research on the effects of the porous structure on diffusion and chemical reactions is necessary. This requires multi-scale models that properly account for the geometry as well as the physical and chemical phenomena at all scales. Nature can be an excellent guide to rational design, as it is full of hierarchical structures that are intrinsically scaling, efficient and robust. This, however, should not reduce to mindless imitation; the biological example needs to be properly chosen, and the different context of technological applications should be accounted for. Thus far, the majority of "biomimetic" research is focused on imitating isolated features of biological structures to synthesize heterogeneous catalysts or constructing flow fields for fuel cells with sub-optimal results. In most cases, the actual physical processes that govern the system are neglected. The examples presented in this paper focused on the utilization of nature-inspired confinement and hierarchically structured

transport networks in porous media for various applications. In following the nature-inspired engineering philosophy, solutions to the above applications were devised by not directly mimicking nature, but rather learning first from it and working within the constraints of each system. Hence, we suggest focusing research on the fundamental understanding of hierarchical structure/function relationships in biological systems. This understanding can then guide the computationally assisted development of novel, nature-inspired hierarchical catalytic nanomaterials and electrochemical devices.

Acknowledgements

The authors gratefully acknowledge support from the EPSRC "Frontier Engineering" Centre for Nature Inspired Engineering (EP/K038656/1).

References

1 M. E. Davis, *Nature*, 2002, **417**, 813–821.
2 C. M. A. Parlett, K. Wilson and A. F. Lee, *Chem. Soc. Rev.*, 2013, **42**, 3876–3893.
3 P. Yang, T. Deng, D. Zhao, P. Feng, D. Pine, B. F. Chmelka, G. M. Whitesides and G. D. Stucky, *Science*, 1998, **282**, 2244–2246.
4 X.-Y. Yang, A. Leonard, A. Lemaire, G. Tian and B.-L. Su, *Chem. Commun.*, 2011, **47**, 2763–2786.
5 Z.-Y. Yuan and B.-L. Su, *J. Mater. Chem.*, 2006, **16**, 663–677.
6 N. Ishizuka, H. Minakuchi, K. Nakanishi, N. Soga and N. Tanaka, *J. Chromatogr. A*, 1998, **797**, 133–137.
7 X. Y. Yang, Z. Q. Li, B. Liu, A. Klein-Hofmann, G. Tian, Y. F. Feng, Y. Ding, D. S. Su and F. S. Xiao, *Adv. Mater.*, 2006, **18**, 410–414.
8 J. R. Greer and W. D. Nix, *Appl. Phys. A: Mater. Sci. Process.*, 2008, **90**, 203.
9 J. Wang, J. Lian, J. R. Greer, W. D. Nix and K.-S. Kim, *Acta Mater.*, 2006, **54**, 3973–3982.
10 O. Wilhelmsson, P. Eklund, F. Giuliani, H. Högberg, L. Hultman and U. Jansson, *Appl. Phys. Lett.*, 2007, **91**, 123124.
11 U. G. K. Wegst, H. Bai, E. Saiz, A. P. Tomsia and R. O. Ritchie, *Nat. Mater.*, 2015, **14**, 23–36.
12 J. Aizenberg and P. Fratzl, *Adv. Mater.*, 2009, **21**, 387–388.
13 D. E. Cameron, C. J. Bashor and J. J. Collins, *Nat. Rev. Microbiol.*, 2014, **12**, 381–390.
14 H. Gao, B. Ji, I. L. Jäger, E. Arzt and P. Fratzl, *Proc. Natl. Acad. Sci. U. S. A.*, 2003, **100**, 5597–5600.
15 H. Kung and M. Kung, *Catal. Lett.*, 2014, **144**, 1643–1652.
16 S. Mann, *Biomineralization: Principles and Concepts in Bioinorganic Materials Chemistry*, Oxford University Press, 2001.
17 L. Marchetti and M. Levine, *ACS Catal.*, 2011, **1**, 1090–1118.
18 O. Paris, I. Burgert and P. Fratzl, *MRS Bull.*, 2010, **35**, 219–225.
19 S. Vogel, *J. Fish Biol.*, 2010, **76**, 1536–1537.
20 P. Fratzl and R. Weinkamer, *Prog. Mater. Sci.*, 2007, **52**, 1263–1334.
21 M.-O. Coppens, *Curr. Opin. Chem. Eng.*, 2012, **1**, 281–289.
22 B. Bhushan and Y. C. Jung, *Prog. Mater. Sci.*, 2011, **56**, 1–108.
23 H. D. Espinosa, J. E. Rim, F. Barthelat and M. J. Buehler, *Prog. Mater. Sci.*, 2009, **54**, 1059–1100.
24 A. Jagota and C.-Y. Hui, *Mater. Sci. Eng., R*, 2011, **72**, 253–292.
25 F. E. Fish, P. W. Weber, M. M. Murray and L. E. Howle, *Integr. Comp. Biol.*, 2011, **51**, 203–213.
26 A. Malshe, K. Rajurkar, A. Samant, H. N. Hansen, S. Bapat and W. Jiang, *CIRP Ann.*, 2013, **62**, 607–628.
27 P. Ball, *Nature*, 1999, **400**, 507–509.
28 L. Wen, J. C. Weaver and G. V. Lauder, *J. Exp. Biol.*, 2014, **217**, 1656–1666.
29 W. Zhang, D. Zhang, T. Fan, J. Gu, J. Ding, H. Wang, Q. Guo and H. Ogawa, *Chem. Mater.*, 2009, **21**, 33–40.
30 L.-C. Sang and M.-O. Coppens, *Phys. Chem. Chem. Phys.*, 2011, **13**, 6689–6698.
31 A. Brinker, G. Pfeifer, M. J. Kerner, D. J. Naylor, F. U. Hartl and M. Hayer-Hartl, *Cell*, 2001, **107**, 223–233.
32 Y. C. Tang, H. C. Chang, K. Chakraborty, F. U. Hartl and M. Hayer-Hartl, *EMBO J.*, 2008, **27**, 1458–1468.
33 A. Brinker, G. Pfeifer, M. J. Kerner, D. J. Naylor, F. U. Hartl and M. Hayer-Hartl, *Cell*, 2001, **107**, 223–233.
34 P. Yang, D. Zhao, D. I. Margolese, B. F. Chmelka and G. D. Stucky, *Nature*, 1998, **396**, 152–155.
35 P. F. Fulvio, S. Pikus and M. Jaroniec, *J. Mater. Chem.*, 2005, **15**, 5049–5053.
36 L.-C. Sang, A. Vinu and M.-O. Coppens, *Langmuir*, 2011, **27**, 13828–13837.
37 A. A. Vertegel, R. W. Siegel and J. S. Dordick, *Langmuir*, 2004, **20**, 6800–6807.
38 J. Siefker, P. Karande and M.-O. Coppens, *Expert Opin. Drug Delivery*, 2014, **11**, 1781–1793.
39 F. Marras, J. Wang, M.-O. Coppens and J. N. H. Reek, *Chem. Commun.*, 2010, **46**, 6587–6589.
40 A. Katz and M. E. Davis, *Nature*, 2000, **403**, 286–289.
41 J. D. Bass, A. Solovyov, A. J. Pascall and A. Katz, *J. Am. Chem. Soc.*, 2006, **128**, 3737–3747.
42 J.-M. Ha, A. Solovyov and A. Katz, *Langmuir*, 2009, **25**, 10548–10553.
43 N. de Silva, J.-M. Ha, A. Solovyov, M. M. Nigra, I. Ogino, S. W. Yeh, K. A. Durkin and A. Katz, *Nat. Chem.*, 2010, **2**, 1062–1068.
44 J.-M. Ha, A. Solovyov and A. Katz, *J. Phys. Chem. C*, 2010, **114**, 16060–16070.
45 M. M. Nigra, A. J. Yeh, A. Okrut, A. G. DiPasquale, S. W. Yeh, A. Solovyov and A. Katz, *Dalton Trans.*, 2013, **42**, 12762–12771.
46 A. Stein, B. E. Wilson and S. G. Rudisill, *Chem. Soc. Rev.*, 2013, **42**, 2763–2803.
47 P. Trogadas, V. Ramani, P. Strasser, T. F. Fuller and M.-O. Coppens, *Angew. Chem., Int. Ed.*, 2016, **55**, 122–148.
48 Y. Liu, J. Goebl and Y. Yin, *Chem. Soc. Rev.*, 2013, **42**, 2610–2653.

49 C. Perego and R. Millini, *Chem. Soc. Rev.*, 2013, **42**, 3956–3976.
50 A. Walcarius, *Chem. Soc. Rev.*, 2013, **42**, 4098–4140.
51 X. Y. Yang, Y. Li, A. Lemaire, J. G. Yu and B. L. Su, *Pure Appl. Chem.*, 2009, **81**, 2265–2307.
52 R. Chal, C. Gérardin, M. Bulut and S. van Donk, *ChemCatChem*, 2011, **3**, 67–81.
53 J. Perez-Ramirez, C. H. Christensen, K. Egeblad, C. H. Christensen and J. C. Groen, *Chem. Soc. Rev.*, 2008, **37**, 2530–2542.
54 M. Kennedy, J. Hu, P. Gao, L. Li, A. Ali-Reynolds, B. Chal, V. Gupta, C. Ma, N. Mahajan, A. Akrami and S. Surapaneni, *Mol. Pharmaceutics*, 2008, **5**, 981–993.
55 K. Pajula, M. Taskinen, V.-P. Lehto, J. Ketolainen and O. Korhonen, *Mol. Pharmaceutics*, 2010, **7**, 795–804.
56 F. Gao, C. Lian, L. Zhou, H. Liu and J. Hu, *Langmuir*, 2014, **30**, 11284–11291.
57 G. F. Froment, K. B. Bischoff and J. de Wilde, *Chemical Reactor Analysis and Design*, John Wiley & Sons, 2011.
58 G. Wang and M.-O. Coppens, *Ind. Eng. Chem. Res.*, 2008, **47**, 3847–3855.
59 M.-O. Coppens, *Structuring catalyst nanoporosity*, Marcel Dekker, 2006.
60 M. Sahimi, G. R. Gavalas and T. T. Tsotsis, *Chem. Eng. Sci.*, 1990, **45**, 1443–1502.
61 M. Loewenberg, *J. Chem. Phys.*, 1994, **100**, 7580–7589.
62 F. J. Keil and C. Rieckmann, *Chem. Eng. Sci.*, 1994, **49**, 4811–4822.
63 F. J. Keil, *Chem. Eng. Sci.*, 1996, **51**, 1543–1567.
64 F. J. Keil, *Catal. Today*, 1999, **53**, 245–258.
65 T. Doğu, *Ind. Eng. Chem. Res.*, 1998, **37**, 2158–2171.
66 S. Mitchell, N.-L. Michels, G. Majano and J. Pérez-Ramírez, *Curr. Opin. Chem. Eng.*, 2013, **2**, 304–311.
67 L. Karwacki, M. H. F. Kox, D. A. Matthijs de Winter, M. R. Drury, J. D. Meeldijk, E. Stavitski, W. Schmidt, M. Mertens, P. Cubillas, N. John, A. Chan, N. Kahn, S. R. Bare, M. Anderson, J. Kornatowski and B. M. Weckhuysen, *Nat. Mater.*, 2009, **8**, 959–965.
68 H. Hu, J. Lyu, Q. Wang, Q. Zhang, J. Cen and X. Li, *RSC Adv.*, 2015, **5**, 32679–32684.
69 M. S. Holm, E. Taarning, K. Egeblad and C. H. Christensen, *Catal. Today*, 2011, **168**, 3–16.
70 S. M. Rao and M.-O. Coppens, *Chem. Eng. Sci.*, 2012, **83**, 66–76.
71 G. Wang and M.-O. Coppens, *Chem. Eng. Sci.*, 2010, **65**, 2344–2351.
72 M. Zhang, C. Shao, Z. Guo, Z. Zhang, J. Mu, P. Zhang, T. Cao and Y. Liu, *ACS Appl. Mater. Interfaces*, 2011, **3**, 2573–2578.
73 L. Zhang, X.-F. Cao, X.-T. Chen and Z.-L. Xue, *J. Colloid Interface Sci.*, 2011, **354**, 630–636.
74 S. Sartipi, K. Parashar, M. Makkee, J. Gascon and F. Kapteijn, *Catal. Sci. Technol.*, 2013, **3**, 572–575.
75 T. Witoon, M. Chareonpanich and J. Limtrakul, *Fuel Process. Technol.*, 2011, **92**, 1498–1505.
76 R. Srivastava, M. Choi and R. Ryoo, *Chem. Commun.*, 2006, 4489–4491.
77 L.-H. Chen, X.-Y. Li, G. Tian, Y. Li, J. C. Rooke, G.-S. Zhu, S.-L. Qiu, X.-Y. Yang and B.-L. Su, *Angew. Chem., Int. Ed.*, 2011, **50**, 11156–11161.
78 S. Gheorghiu and M.-O. Coppens, *AIChE J.*, 2004, **50**, 812–820.
79 G. Wang, E. Johannessen, C. R. Kleijn, S. W. de Leeuw and M.-O. Coppens, *Chem. Eng. Sci.*, 2007, **62**, 5110–5116.
80 P. Kortunov, S. Vasenkov, J. Kärger, M. Fé Elía, M. Perez, M. Stöcker, G. K. Papadopoulos, D. Theodorou, B. Drescher, G. McElhiney, B. Bernauer, V. Krystl, M. Kočiřík, A. Zikánová, H. Jirglová, C. Berger, R. Gläser, J. Weitkamp and E. W. Hansen, *Chem. Mater.*, 2005, **17**, 2466–2474.
81 A. El Kadib, R. Chimenton, A. Sachse, F. Fajula, A. Galarneau and B. Coq, *Angew. Chem., Int. Ed.*, 2009, **48**, 4969–4972.
82 J. Babin, J. Iapichella, B. Lefevre, C. Biolley, J.-P. Bellat, F. Fajula and A. Galarneau, *New J. Chem.*, 2007, **31**, 1907–1917.
83 J. C. Groen, W. Zhu, S. Brouwer, S. J. Huynink, F. Kapteijn, J. A. Moulijn and J. Pérez-Ramírez, *J. Am. Chem. Soc.*, 2007, **129**, 355–360.
84 M. Choi, H. S. Cho, R. Srivastava, C. Venkatesan, D.-H. Choi and R. Ryoo, *Nat. Mater.*, 2006, **5**, 718–723.
85 G. Ye, X. Duan, K. Zhu, X. Zhou, M.-O. Coppens and W. Yuan, *Chem. Eng. Sci.*, 2015, **132**, 108–117.
86 P. Forte, A. Sachse, M. Maes, A. Galarneau and D. De Vos, *RSC Adv.*, 2014, **4**, 1045–1054.
87 A. Sachse, A. Galarneau, F. Fajula, F. Di Renzo, P. Creux and B. Coq, *Microporous Mesoporous Mater.*, 2011, **140**, 58–68.
88 A. Sachse, A. Merceille, Y. Barré, A. Grandjean, F. Fajula and A. Galarneau, *Microporous Mesoporous Mater.*, 2012, **164**, 251–258.
89 F. J. Keil and C. Rieckmann, *Hung. J. Ind. Chem.*, 1993, **21**, 277–286.
90 C. Rieckmann, T. Düren and F. J. Keil, *Hung. J. Ind. Chem.*, 1997, **25**, 137–145.
91 B. J. Smith and J. Wei, *J. Catal.*, 1991, **132**, 41–57.
92 G. Ye, X. Zhou, M.-O. Coppens and W. Yuan, *AIChE J.*, 2015, **62**, 451–460.
93 A. J. J. Koekkoek, H. Xin, Q. Yang, C. Li and E. J. M. Hensen, *Microporous Mesoporous Mater.*, 2011, **145**, 172–181.
94 M. Hartmann, *Angew. Chem., Int. Ed.*, 2004, **43**, 5880–5882.
95 C. H. Christensen, K. Johannsen, I. Schmidt and C. H. Christensen, *J. Am. Chem. Soc.*, 2003, **125**, 13370–13371.
96 M.-O. Coppens, *Ind. Eng. Chem. Res.*, 2005, **44**, 5011–5019.
97 S. Kjelstrup, M.-O. Coppens, J. G. Pharoah and P. Pfeifer, *Energy Fuels*, 2010, **24**, 5097–5108.
98 B. Ramos-Alvarado, A. Hernandez-Guerrero, F. Elizalde-Blancas and M. W. Ellis, *Int. J. Hydrogen Energy*, 2011, **36**, 12965–12976.

